Supplementary to "Joint evolution of irrigation, the water cycle and water resources under a strong climate change scenario from 1950 to 2100 in the IPSL-CM6"

Pedro Felipe Arboleda-Obando[1,2], Agnès Ducharne[1,2], Frédérique Cheruy[2,3], Josefine Ghattas[2]

[1]Laboratoire METIS (umr 7619), IPSL, Sorbonne Université, CNRS, EPHE, 75005 Paris, France
[2]Institut Pierre Simon Laplace (FR 636, Sorbonne Université, CNRS), Paris, France
[3]Laboratoire de Météorologie Dynamique (UMR 8539, Sorbonne Université, CNRS), Paris, France

We present here the supplementary material to the paper "Joint evolution of irrigation, water cycle and water resources under a strong climate change scenario from 1950 to 2100 in the IPSL-CM6". Figure S1 shows the spatial distribution of cropland fraction in the future (2050-2100) and the change of cropland fraction in the future compared to the historical period (1950-2000). Figure S2 shows the evolution of cropland area and irrigated area (S2-a), the evolution of the ratio of irrigated area and cropland area (S2-b), and the evolution of cropland area by continent (S2-c). These two plots complete the description of main characteristics of the scenario SSP5-8.5 on land use changes.

Figure S3 shows the effect of climate change and the influence of irrigation on precipitation and air temperature, including the oceans. Fig S4 shows the influence of irrigation on climate change effects in evapotranspiration (ET), precipitation (P), groundwater (GW) reservoir and Stream reservoir. This information is important to understand the evolution of irrigation influence on different fluxes and storage variables.

Fig. S5 shows the time-series at global, irrigated areas and non-irrigated areas for total runoff (R) and leaf area index (LAI), and S6 shows the irrigation influence in the future and irrigation influence on climate change effects, for both variables. Must be noted that the influence of irrigation on total runoff follows the spatial patterns of irrigation influence on precipitation; for leaf area index, the spatial distribution follows the spatial distribution of irrigation influence on evapotranspiration.

FIg. S7 and S8 show the same information as S5 and S6 for soil moisture and total water storage (TWS). Irrigation influence is positive for both variables in irrigated areas, but is much weaker for TWS, while in general irrigation influence on climate change effects is weak for both variables. Finally, S9 and S10 show the same information for air temperature and net radiation. The irrigation influence is important for both variables in irrigated, but irrigation influence on climate change effects are weak and in many areas, non-significant.

Table S1 shows information of large river basins where river discharge at the basin mouth between Irr and NoIrr simulations were compared. We included information of the basin area at the model's resolution, and information of irrigated fraction, discharge for the Irr simulation, and irrigation influence (i.e. Irr-NoIrr) on river discharge for historical and future climates.

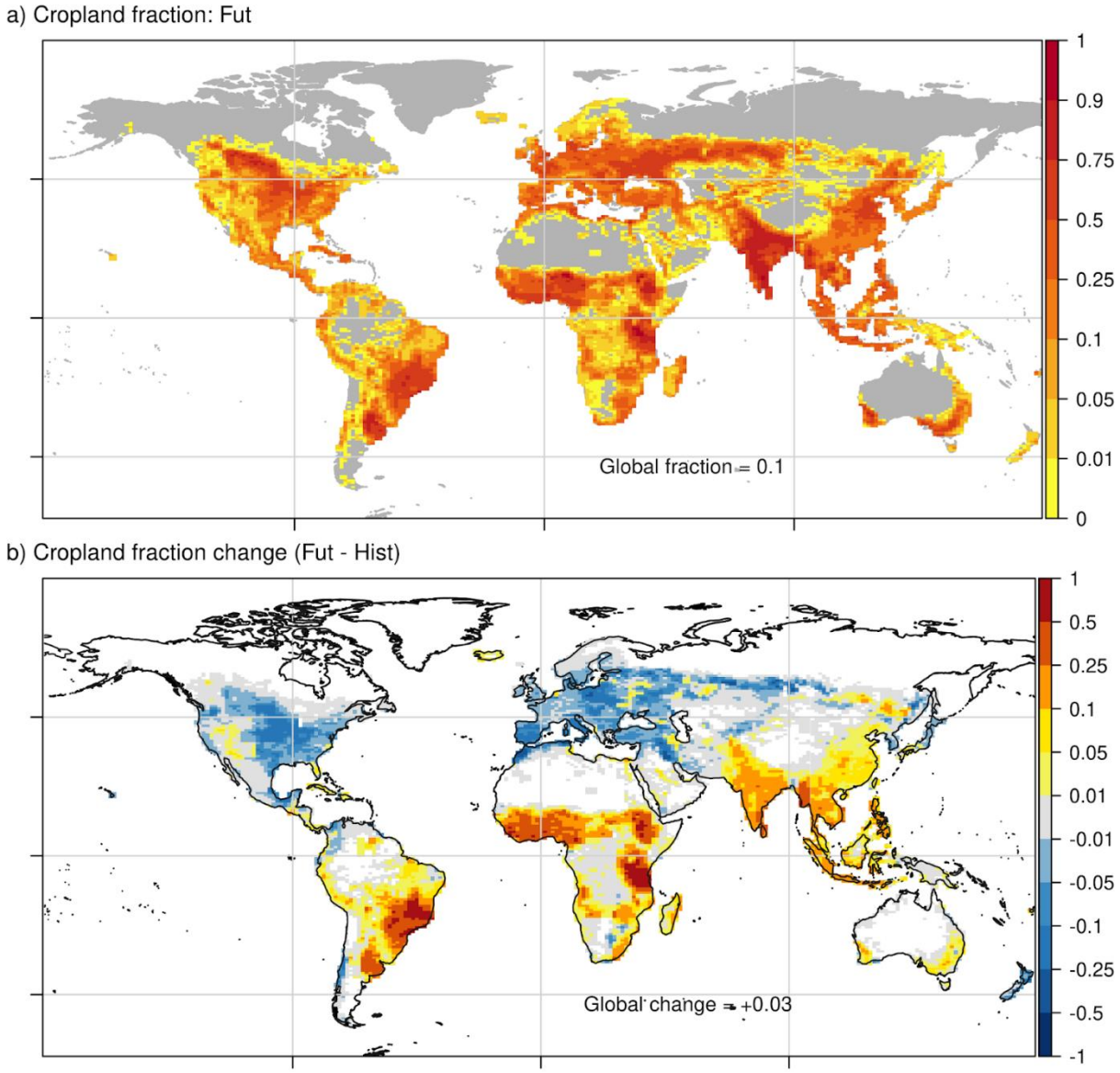

Fig. S1. (a) Map of average cropland fraction by grid cell for the future period (2050-2100). (b) Map of change of average cropland fraction by grid cell between future (2050-2100) and historic (1950-2000) period. Cropland fractions are prescribed by LUHv2 dataset and interpolated to the model resolution.

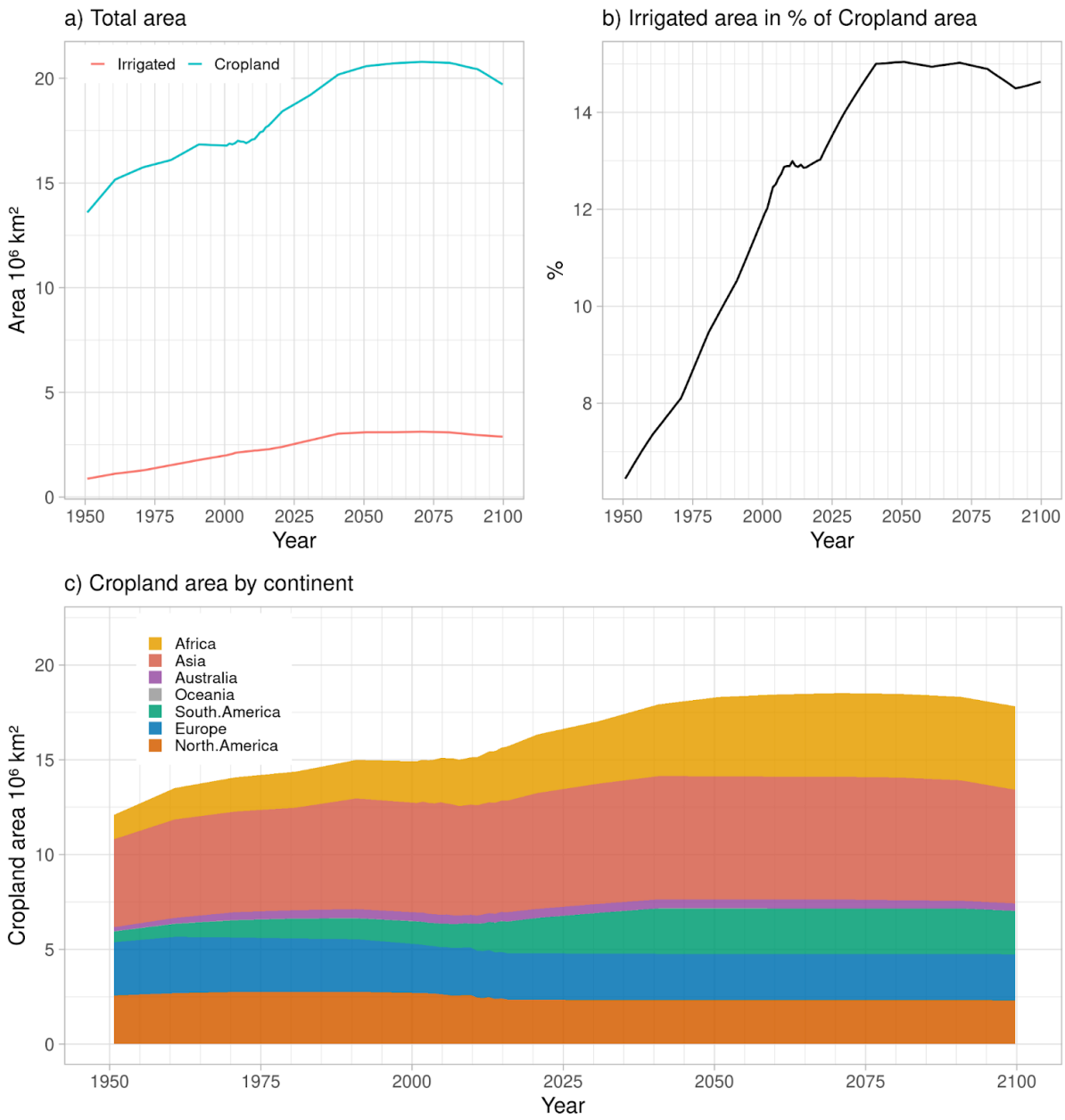

Fig. S2. (a) Total cropland area and irrigated area at global scale. (b) ratio of irrigated fraction and cropland fraction, in percent. (c) Irrigated area by continent prescribed by LUHv2.

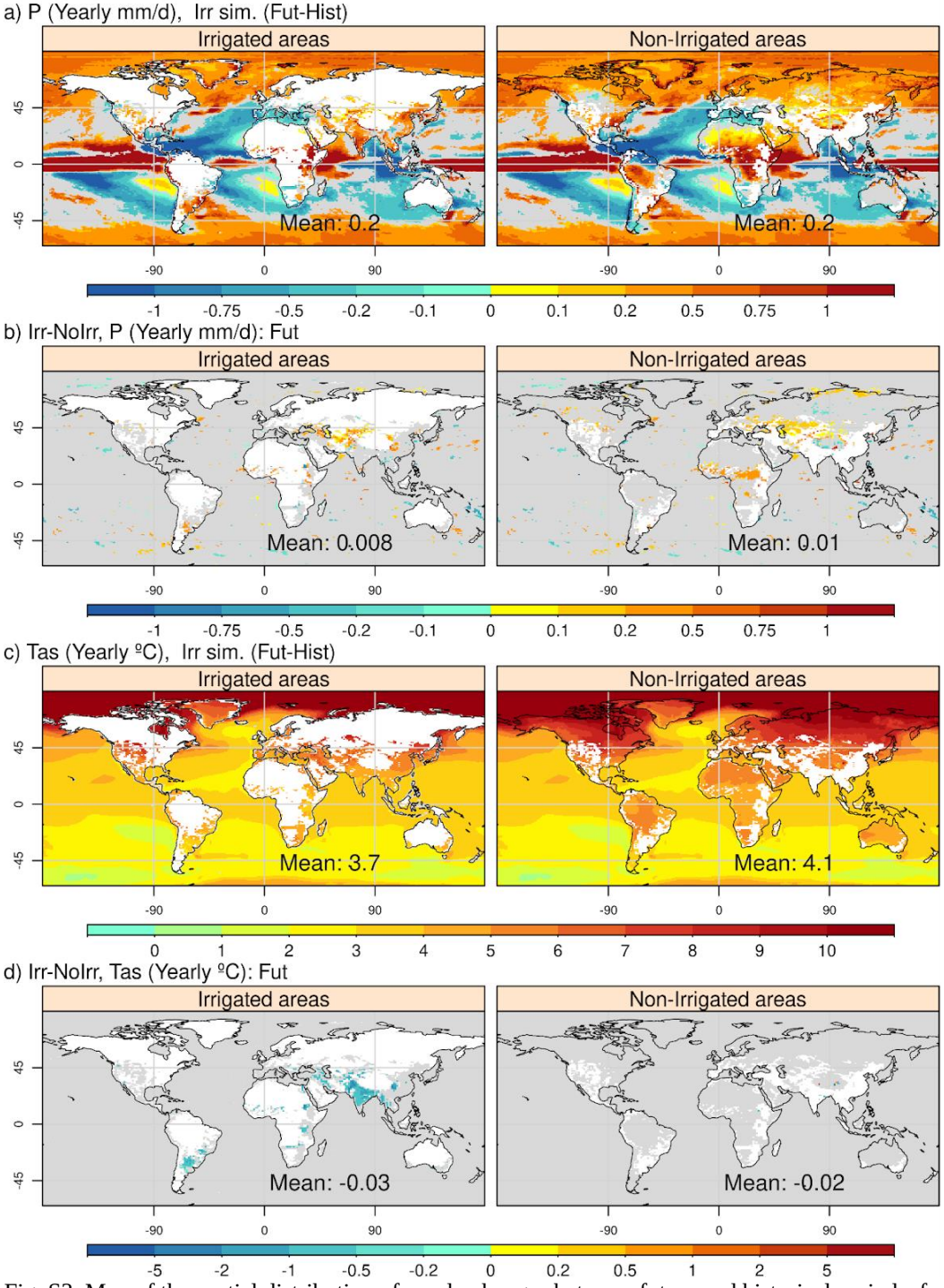

Fig. S3. Map of the spatial distribution of yearly changes between future and historical periods, for irrigated areas and the ocean (left column) and for non-irrigated areas and the ocean (right column) for precipitation (a) and air temperature (c). Map of the spatial distribution of yearly changes between Irr and NoIrr simulation under future climate, for irrigated areas

(left column) and non-irrigated areas (right column) for precipitation (b) and air temperature (d). Areas in gray correspond to a p value under 0.05 according to a Student's t-test are shown.

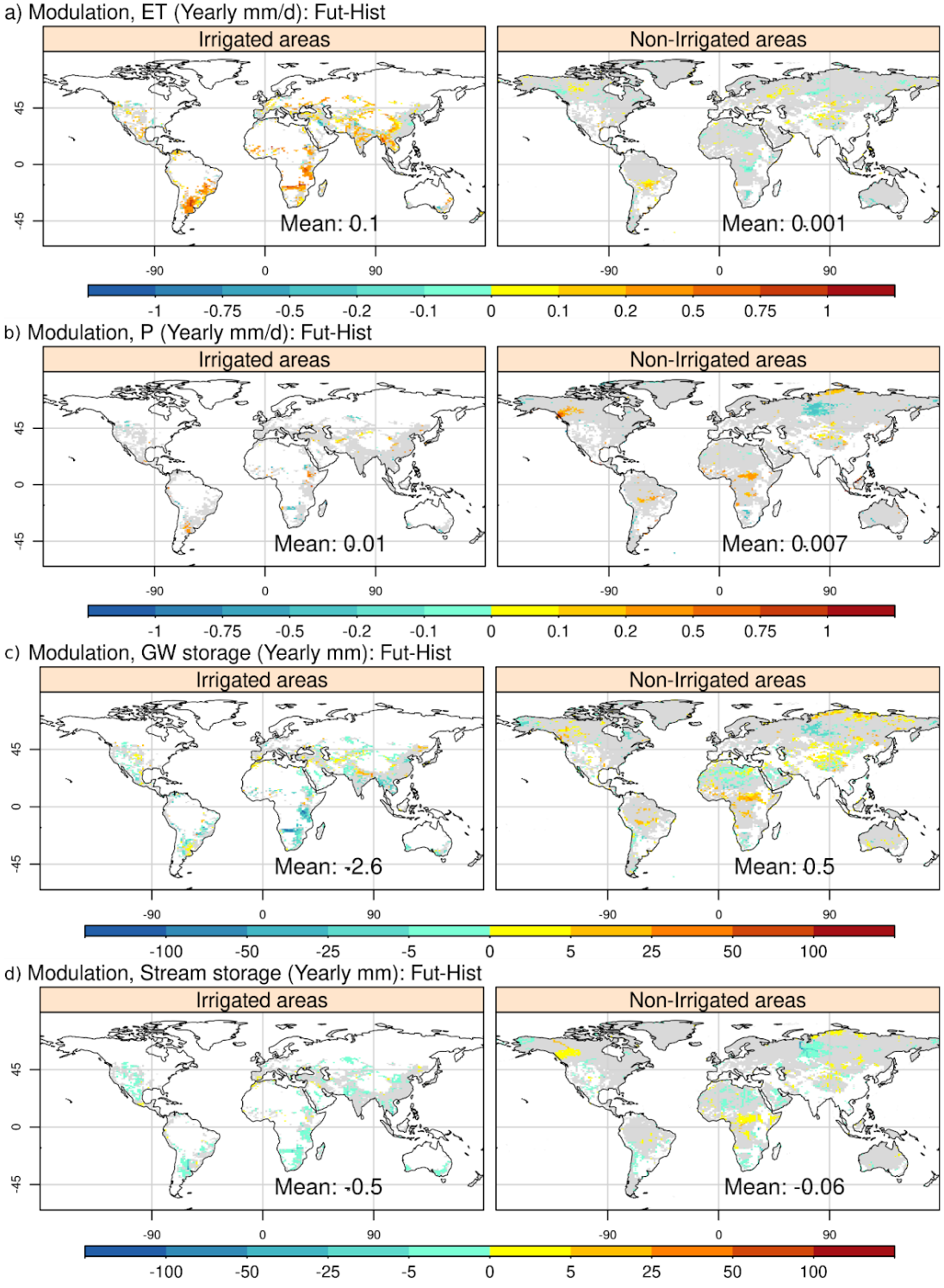

Fig. S4. Map of the spatial distribution of yearly changes between Irr-NoIrr under future climate and Irr-NoIrr under historical climate, for irrigated areas (left column) and non-irrigated areas (right column) for evapotranspiration (a) precipitation (b), groundwater reservoir (c) and stream reservoir (d). Areas in gray correspond to a p value under 0.05 according to a Student's t-test are shown.

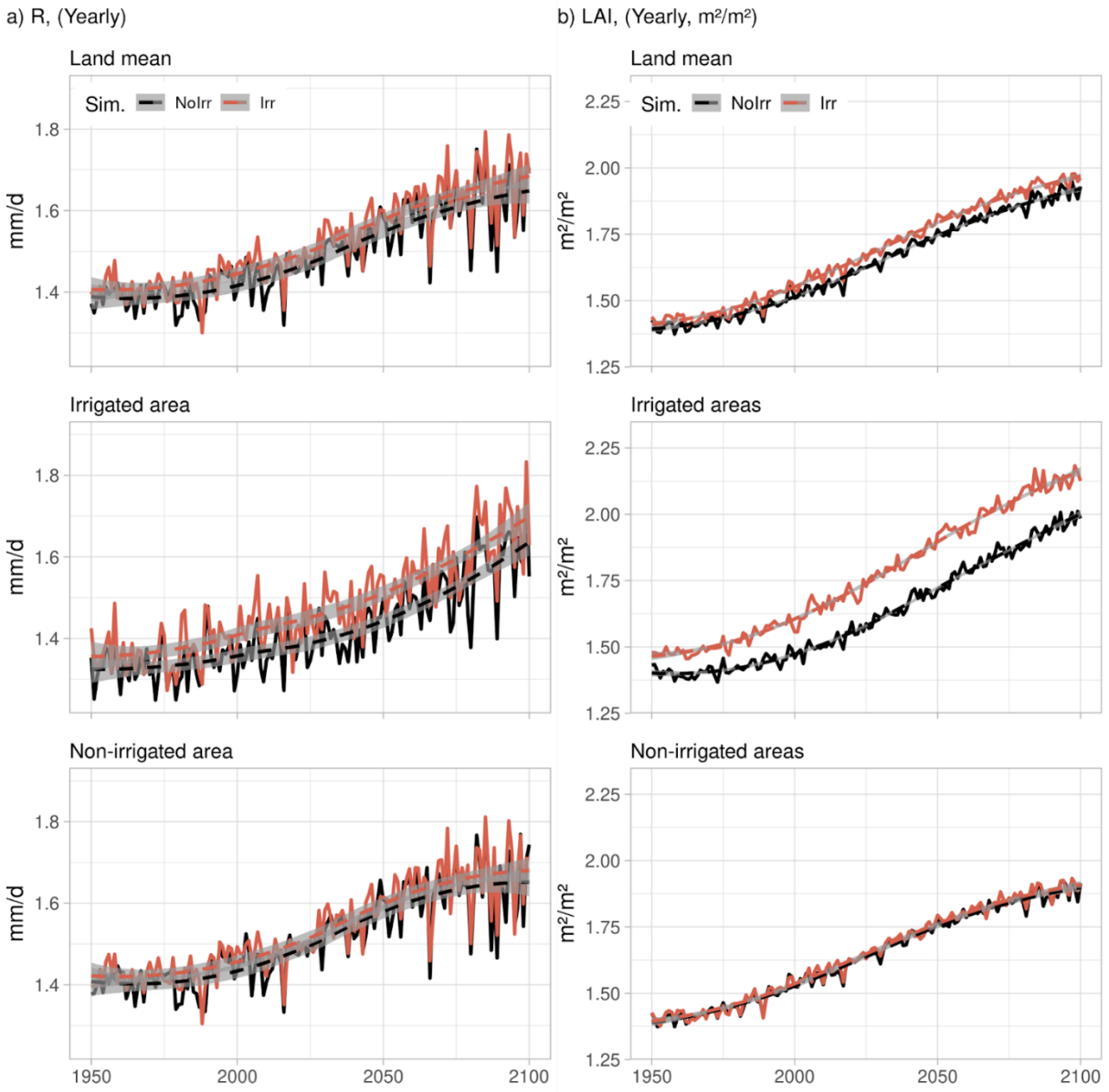

Fig. S5. Yearly time series of total runoff (a, left column) and leaf area index (b, right column). First row corresponds to average on land, second row corresponds to average in irrigated areas, third row corresponds to average in non-irrigated areas. Lines correspond to fitted polynomial surface using local fitting.

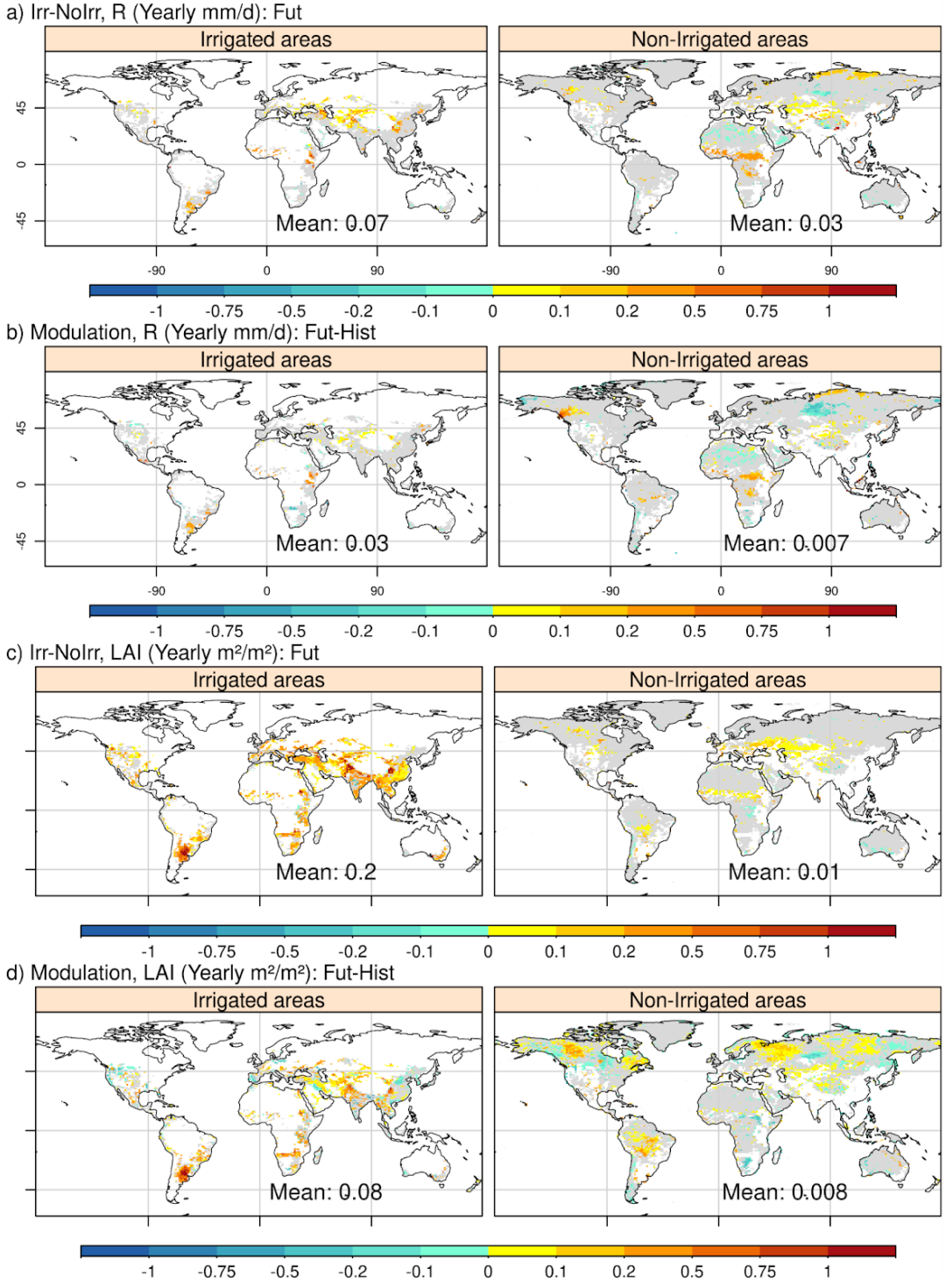

Fig. S6. Map of the spatial distribution of yearly changes between Irr and NoIrr simulation under future climate, for irrigated areas (left column) and non-irrigated areas (right column) for total runoff (a) and leaf area index (c). Map of the spatial

distribution of yearly changes between Irr-NoIrr under future climate and Irr-NoIrr under historical climate, for total runoff (b) and leaf area index (d). Areas in gray correspond to a p value under 0.05 according to a Student's t-test are shown.

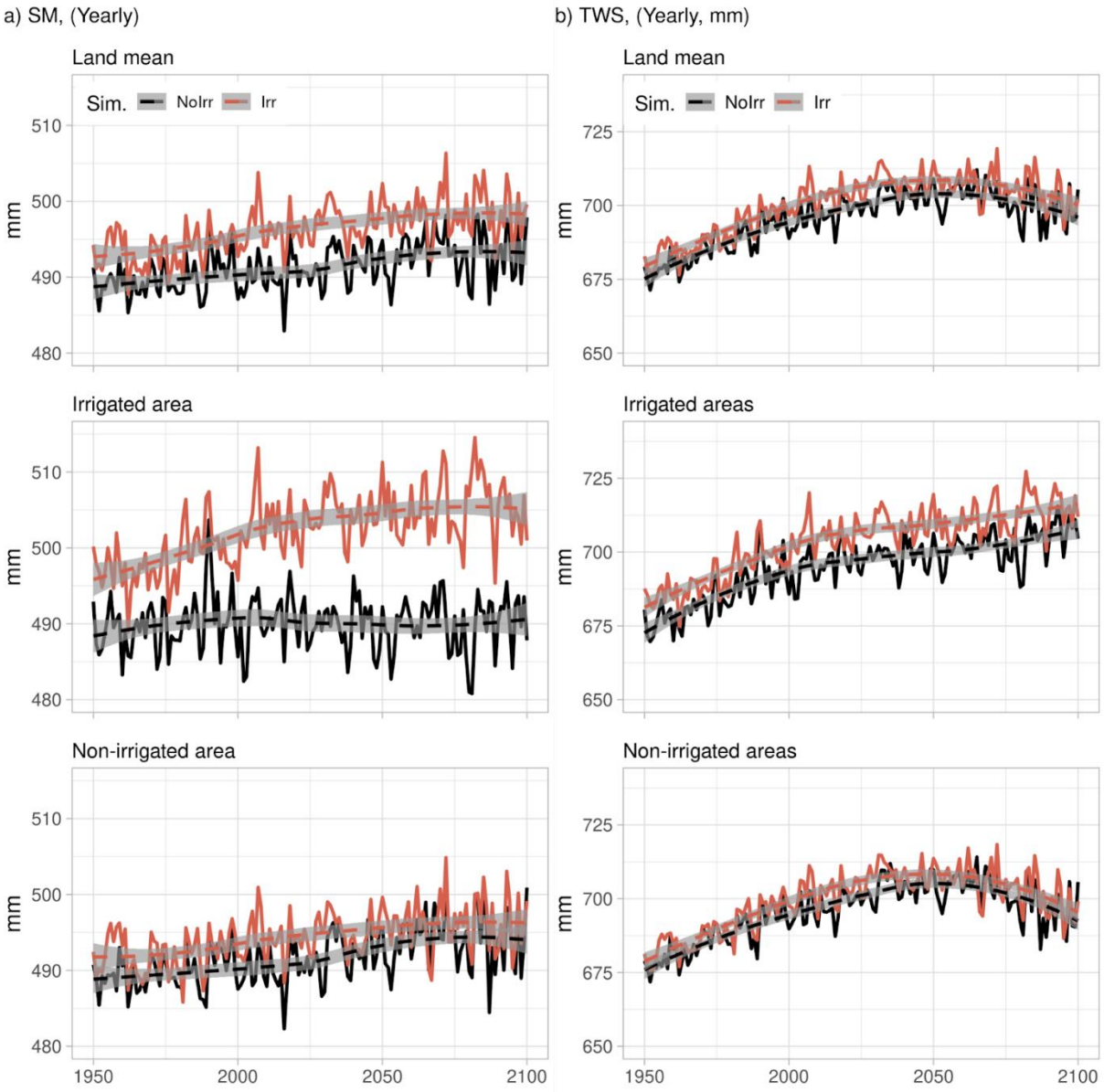

Fig. S7. Yearly time series of soil moisture (a, left column) and total water storage (b, right column). First row corresponds to average on land, second row corresponds to average in irrigated areas, third row corresponds to average in non-irrigated areas. Lines correspond to fitted polynomial surface using local fitting.

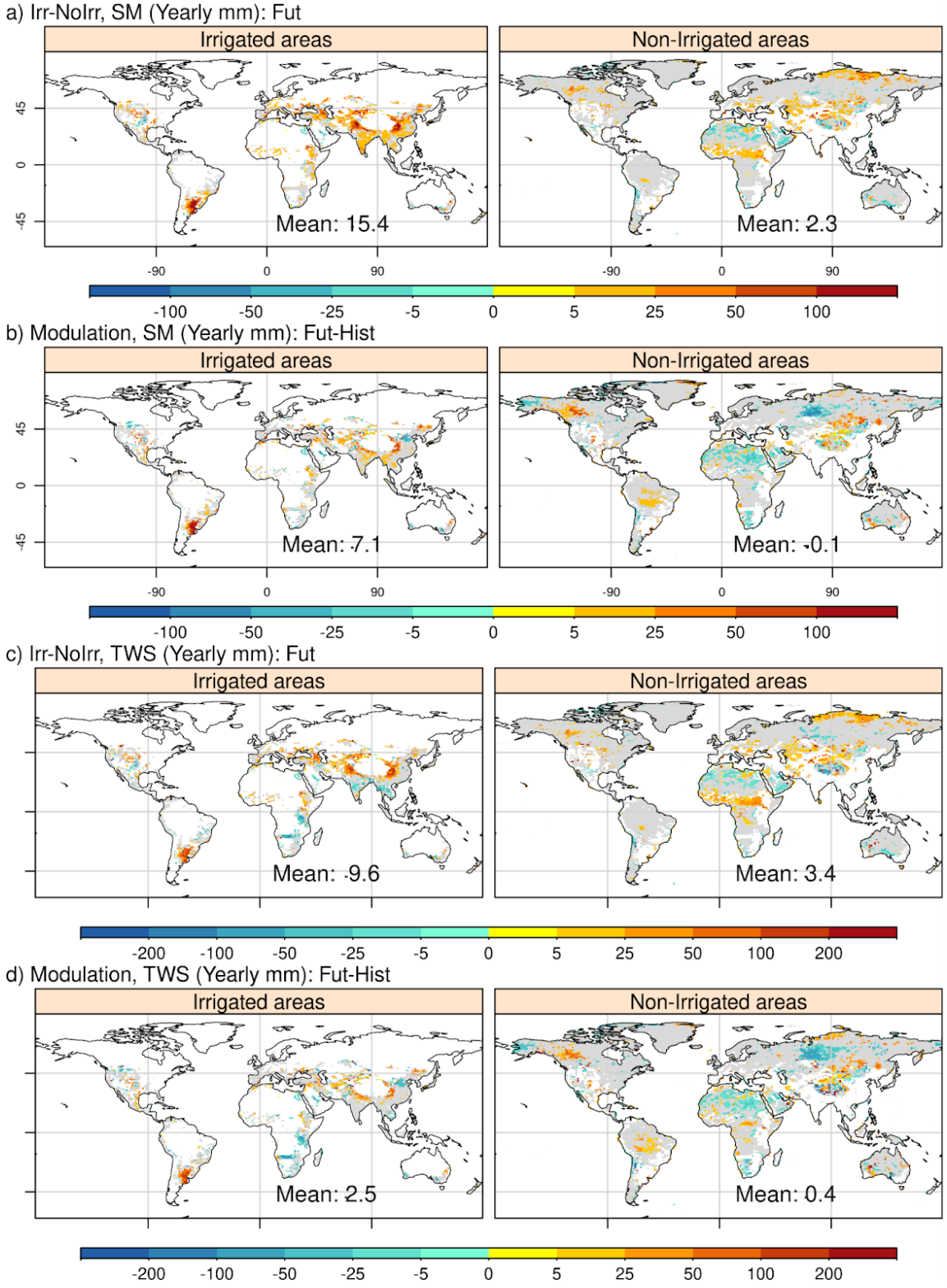
a) Irr-NoIrr, SM (Yearly mm): Fut
Irrigated areas
Non-Irrigated areas
Mean: 15.4
Mean: 2.3
b) Modulation, SM (Yearly mm): Fut-Hist
Mean: 7.1
Mean: -0.1
c) Irr-NoIrr, TWS (Yearly mm): Fut
Mean: -9.6
Mean: 3.4
d) Modulation, TWS (Yearly mm): Fut-Hist
Mean: 2.5
Mean: 0.4
45
0
-45
-90
0
90
-100
-50
-25
-5
0
5
25
50
100
-200
200

Fig. S8. Map of the spatial distribution of yearly changes between Irr and NoIrr simulation under future climate, for irrigated areas (left column) and non-irrigated areas (right column) for soil moisture (a) and total water storage (c). Map of the spatial distribution of yearly changes between Irr-NoIrr under future climate and Irr-NoIrr under historical climate, for soil moisture (b) and total water storage (d). Areas in gray correspond to a p value under 0.05 according to a Student's t-test are shown.

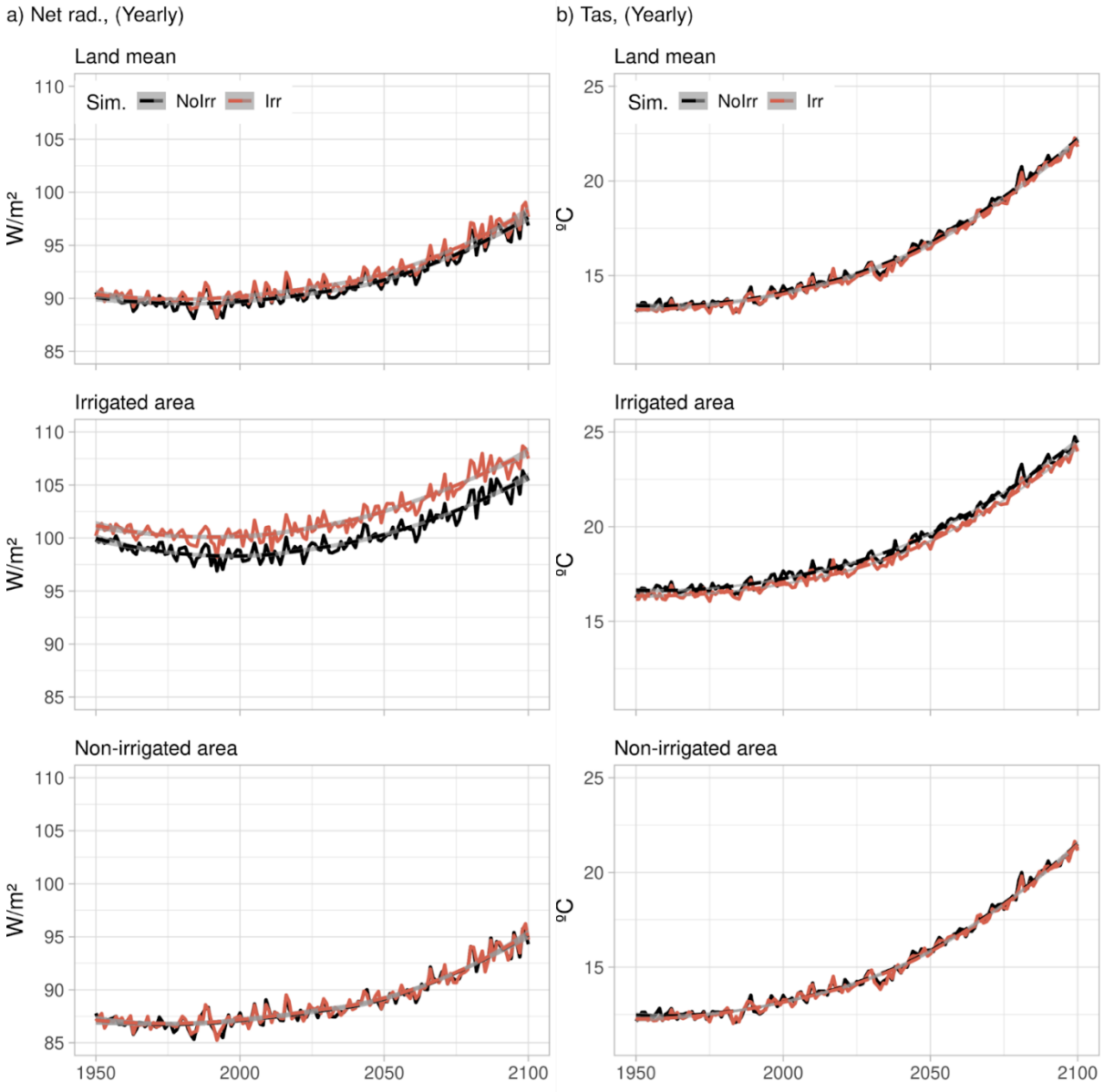

Fig. S9. Yearly time series of net radiation (a, left column) and air temperature at 2m (b, right column). First row corresponds to average on land, second row corresponds to average in irrigated areas, third row corresponds to average in non-irrigated areas. Lines correspond to fitted polynomial surface using local fitting.

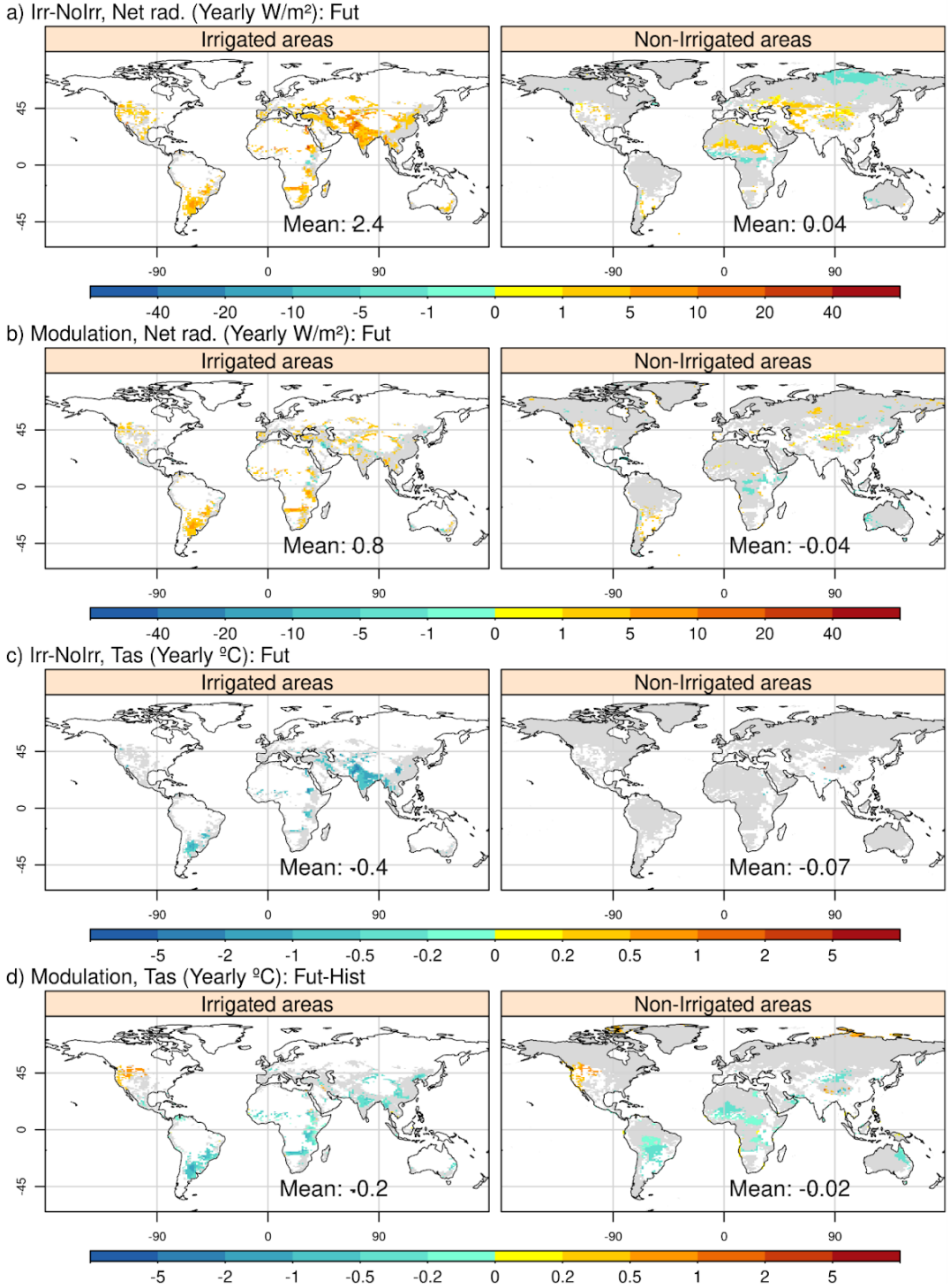

Fig. S10. Map of the spatial distribution of yearly changes between Irr and NoIrr simulation under future climate, for irrigated areas (left column) and non-irrigated areas (right column) for net radiation (a) and air temperature at 2m (c). Map of the spatial distribution of yearly changes between Irr-NoIrr under future climate and Irr-NoIrr under historical climate, for

net radiation (b) and air temperature at 2m (d). Areas in gray correspond to a p value under 0.05 according to a Student's t-test are shown.

Table S1. Average values of irrigated fraction, river discharge, and irrigation influence for 50 large river basins, under historical and future climate. Values in bold with * correspond to a p value under 0.05. River basins used for analysis in the document are highlighted in yellow. Colors indicate basins classified according to classes in the main document: first class (red, heavy irrigation activities), second class (green, modest irrigation activities, negative climate change impact) third class (yellow, few irrigation activities, positive irrigation influence) and unclassified (no color).

Id.	Basin	Area km² 10^6	Hist (1950-2000)			Fut (2050-2100)		
			Irr. frac (%)	Qirr m³/s	Irr-NoIrr (%)	Irr. frac (%)	Qirr m³/s	Irr-NoIrr (%)
1	Lena	2.62	0.00	17568.8	3.4	0.00	24723.7	1.3
2	Yenisei	2.72	0.00	19980.0	4.7	0.02	24216.4	-0.3
3	Mackenzie	2.01	0.00	11032.4	-4.4	0.00	13638.5	5.3
4	Kolyma	0.76	0.00	4615.3	6.2	0.00	8715.0	5.4
5	Ob	2.99	0.07	18461.5	8.3	0.23	18547.2	**-8.7***
6	Yukon	1.10	0.00	9591.0	2.3	0.00	14223.7	-0.5
7	Nelson	1.23	0.27	5292.1	**10.4***	0.42	4631.2	4.4
8	Amur	3.26	0.56	14525.1	**-8.8***	1.91	20437.6	-1
9	St. Lawrence	1.22	0.01	15243.3	3.5	0.01	16153.2	0.9
10	Dnepr	0.69	0.42	3759.4	1.6	0.74	3434.0	-4.4
11	Volga	1.76	0.12	11341.8	-3	0.16	13217.6	-2.5
12	Columbia	0.86	2.31	10120.2	-1.3	2.62	8677.9	**-9.2***
13	Syr-Darya	1.22	2.02	3220.6	**-12.6***	2.21	4071.4	**-14.3***
14	Danube	0.93	0.34	8023.8	0.6	0.56	6692.9	**-6.1***
15	Amu-Darya	0.78	4.38	4084.3	**-25.8***	6.29	4960.0	**-22.8***
16	Tarim	0.85	0.69	2702.6	-5.7	1.57	3240.8	-7.7
17	Huang He	1.06	7.57	1740.3	**-34.1***	11.39	2624.4	**-34.1***
18	Chott Jerid	0.89	0.00	223.9	0.4	0.01	253.7	**-19.1***
19	Colorado Ari	1.03	0.66	1599.5	**-19.3***	1.07	1370.8	**-34.4***

20	Chang Jiang Yangtze	2.00	7.13	21416.4	**-7.9***	12.54	23189.1	**-9.3***
21	Nile	4.19	0.63	17365.5	**-10.6***	2.42	33768.2	**-8.1***
22	Mississippi	3.49	3.07	21605.4	-4.5	3.23	25184.6	-4.5
23	Wadi al Farigh	0.83	0.00	35.5	**16.1***	0.01	117.1	**-12.2***
24	GHAASBasin51	0.55	0.03	27.9	**86.3***	0.07	118.6	**-10.3***
25	Shatt el Arab	1.28	2.63	3776.3	**-33.1***	3.32	4606.3	**-18.5***
26	Rio Grande US	1.01	0.79	806.3	**-49***	1.20	1081.8	**-51.8***
27	GHAASBasin61	0.65	0.29	188.0	**-29.8***	0.60	302.1	**-39.4***
28	Indus	1.29	10.61	4766.2	**-52.5***	17.66	6644.8	**-49.4***
29	Ganges	1.91	8.96	31014.9	**-15.2***	23.16	40441.8	**-11.9***
30	Zhujiang	0.55	2.78	7691.2	-3.7	8.75	8652.2	-3.6
31	Erg Iguidi Sahara	2.07	0.01	318.6	**-7.8***	0.01	651.4	**-12.3***
32	GHAASBasin50	0.55	0.41	270.6	**-32.5***	0.73	575.2	**-32.6***
33	Senegal	0.97	0.03	1360.9	0.6	0.07	2181.9	**11.2***
34	Komadugu Yobe Tchad	0.73	0.05	527.2	1.3	0.16	2280.2	**-12.5***
35	Chari	1.59	0.01	4928.5	**13.5***	0.07	12898.5	5.7
36	Mekong	1.17	1.14	15841.8	**-7.6***	4.96	17153.8	**-13.9***
37	Orinoco	1.22	0.26	53704.1	1.1	0.68	45400.2	0.3
38	Niger	2.58	0.06	14190.6	**7.7***	0.16	23717.4	3.2
39	Jubba	1.12	0.03	9441.0	6.2	1.12	21473.6	**8.8***
40	Amazon	6.22	0.15	192666.5	-0.3	0.22	216128.7	0.7
41	Tocantins	0.86	0.06	17407.1	-2.9	0.23	18720.6	-1.9
42	Congo	3.98	0.00	80971.5	2.5	0.53	120569.3	**4.3***
43	Sao Francisco	0.80	0.11	5390.5	-7.5	0.34	5524.7	**-17***
44	Zambezi	2.37	0.01	34015.4	2.6	3.12	30111.6	**-15.7***
45	Limpopo	0.54	0.56	1371.2	**-24.2***	3.34	1268.2	**-47.9***

46	Orange	0.94	0.34	3906.1	4.8	1.96	3102.6	**-23.3***
47	Great Artesian Basin	1.24	0.00	4389.8	0.7	0.00	4271.4	-1.2
48	Parana	3.01	0.27	27081.5	-3.6	3.25	28821.6	**-16.7***
49	Murray	1.35	0.63	3276.4	**-20.3***	2.43	2658.6	**-41.1***
50	Colorado Arg	0.66	0.51	606.7	**-38.5***	1.87	607.3	**-50.2***

105